tvst

Article

Integrating Differential Gene Expression Analysis with Perturbagen-Response Signatures May Identify Novel Therapies for Thyroid-Associated Orbitopathy

John Y. Lee[1], Ryan A. Gallo[1], Paul J. Ledon[1], Wensi Tao[2], David T. Tse[1], Daniel Pelaez[1], and Sara T. Wester[1]

[1] Dr. Nasser Al-Rashid Orbital Vision Research Center, Bascom Palmer Eye Institute, Department of Ophthalmology, University of Miami Miller School of Medicine, Miami, Florida, USA
[2] Department of Radiation Oncology, University of Miami Miller School of Medicine, Miami, Florida, USA

Correspondence: Daniel Pelaez, Department of Ophthalmology, Bascom Palmer Eye Institute, McKnight Vision Research Center, University of Miami School of Medicine, Room 804, 1638 NW 10th Ave, Miami, FL 33136, USA. e-mail: dpelaez@med.miami.edu
Sara T. Wester, Department of Ophthalmology, Bascom Palmer Eye Institute, 900 NW 17th St., Miami, FL 33136, USA. e-mail: swester2@med.miami.edu

Received: April 22, 2020
Accepted: July 10, 2020
Published: August 25, 2020

Keywords: thyroid-associated orbitopathy; thyroid eye disease; Graves' ophthalmopathy; orbital adipose stem cells; LINCS; adipogenesis

Citation: Lee JY, Gallo RA, Ledon PJ, Tao W, Tse DT, Pelaez D, Wester ST. Integrating differential gene expression analysis with perturbagen-response signatures may identify novel therapies for thyroid-associated orbitopathy. Trans Vis Sci Tech. 2020;9(9):39, https://doi.org/10.1167/tvst.9.9.39

Purpose: To evaluate the efficacy of Library of Integrated Network-based Cellular Signatures (LINCS) perturbagen prediction software to identify small molecules that revert pathologic gene signature and alter disease phenotype in orbital adipose stem cells (OASCs) derived from patients with thyroid-associated orbitopathy (TAO).

Methods: Differentially expressed genes identified via RNA sequencing were inputted into LINCS L1000 Characteristic Direction Signature Search Engine (L1000CDS^2) to predict candidate small molecules to reverse pathologic gene expression. TAO OASC cell lines were treated in vitro with six identified small molecules (Torin-2, PX12, withaferin A, isoliquiritigenin, mitoxantrone, and MLN8054), and expression of key adipogenic and differentially expressed genes was measured with quantitative polymerase chain reaction after 7 days of treatment. OASCs were differentiated into adipocytes, treated for 15 days, and stained with Oil Red O (OD 490 nm) to evaluate adipogenic changes.

Results: The expression of key differentially expressed genes (IRX1, HOXB2, S100B, and KCNA4) and adipogenic genes (peroxisome proliferator activated receptor-γ, FABP4) was significantly decreased in TAO OASCs after treatment ($P < .05$). In treated TAO adipocytes ($n = 3$), all six tested small molecules yielded significant decrease ($P < .05$) in Oil Red O staining. In treated non-TAO adipocytes ($n = 3$), only three of the drugs yielded a significant decrease in Oil Red O staining.

Conclusions: Combining disease expression signatures with LINCS small molecule prediction software can identify promising preclinical drug candidates for TAO.

Translational Relevance: These findings may offer insight into future potential therapeutic options for TAO and demonstrate a streamlined model to predict drug candidates for other diseases.

Introduction

Thyroid-associated orbitopathy (TAO), also known as thyroid eye disease or Graves' ophthalmopathy, is an autoimmune disease with significant orbital complications, including exophthalmos, strabismus, diplopia, and in severe cases, compressive optic neuropathy.[1,2] Until recently, there has been no therapy approved by the US Food and Drug Administration for TAO, and medical management has been traditionally performed with corticosteroids, immunomodulation,

and/or external beam radiation.[3] Unfortunately, these treatment options provide variable degrees of success with high relapse rates, side effects, and risks. Significant research has recently been focused on improving treatment options for TAO, and therapeutic candidates such as teprotumumab (human monoclonal antibody inhibitor of insulin growth factor 1 receptor) have demonstrated promising results, leading to US Food and Drug Administration approval of this medication in January of 2020.[4–6]

In line with these therapeutic advancements, expanding treatment strategies beyond immune-based modalities may provide additional efficacious and potentially synergistic treatment options for patients with TAO. Aside from the autoimmune dysregulation that is inherent to this disease, TAO orbital adipose stem cells (OASCs) possess a unique gene expression profile with 54 differentially expressed genes (DEGs) compared with their non-TAO counterparts.[7] This unique gene expression signature may contribute to components of underlying disease pathology, such as upregulated adipogenesis and inflammation. Thus, developing molecular, gene-based treatment options that can selectively revert differential gene expression in these cells may prove to be an effective treatment approach.

The Library of Integrated Network-based Cellular Signatures (LINCS) provides a unique opportunity to streamline the identification of preclinical drug candidates, as a consortium funded by the National Institutes of Health that has generated an extensive reference library of cell-based perturbagen-response signatures.[8,9] The LINCS L1000CDS^2 software can calculate and generate a ranked list of small molecules predicted to either upregulate or downregulate expression of specified genes, based on a transcriptional response database of reference small molecules. As a relatively recent bioinformatic tool, the LINCS dataset has been used extensively in oncology to identify drug candidates and has yet to be applied for TAO.[10–12] Therefore, we hypothesize that integrating the TAO-specific gene signature from OASCs with the LINCS dataset can yield novel preclinical drug candidates for TAO. In this study, we identify and evaluate the efficacy of LINCS-predicted small molecules to revert the disease signature in TAO OASCs and demonstrate corresponding adipogenic changes in vitro.

Methods

Participants and Specimen Collection

Orbital adipose tissue was harvested from patients with TAO undergoing orbital decompression surgery for orbital rehabilitation or compressive optic neuropathy at the Bascom Palmer Eye Institute. Control orbital fat samples were obtained from patients undergoing blepharoplasty procedures from the medial upper eyelid or lower eyelid fat pads, which are contiguous with the orbital fat and derived from the same embryonic lineage.[13] Patients with a history of orbital trauma, endophthalmitis, surgery (excluding strabismus surgery), or orbital radiation were excluded. Three patients with TAO and three control patients were included from the study (Table 1). Patient records were reviewed to identify demographic information, disease activity and severity (clinical activity score [CAS]), past medical and surgical treatment history for thyroid disease, systemic corticosteroid therapy, and smoking history. Collection of protected patient health information was compliant with the rules and regulations of the Health Insurance Portability and Accountability Act, and Institutional Review Board approval was obtained by the University of Miami Human Studies Committee. Informed consent was obtained from each participant to use tissue for research purposes. All procedures performed in this study involving human participants were in accordance with the ethical standards of the institutional research committee and the 1964 Declaration of Helsinki.

OASC Isolation and Culture

OASCs were isolated as described previously from patients with and without TAO.[7,14] Orbital fat samples were cut into sections less than 5 mm in size. Adipose tissue was digested with 1 mg/mL Col I (Worthington Biochemical Corp, Lakewood, NJ) in Dulbecco's modified Eagle's medium (DMEM) for 3 hours on a shaker. Digested tissue was pipetted up and down at least 10 times before centrifugation at 300*g* for 5 minutes to remove floating adipocytes. Pellets were suspended in DMEM and filtered with a 70 µm nylon strainer (BD Bioscience, Franklin Lakes, NJ) to yield flow-through cells as stromal vascular fraction. Cells in the stromal vascular fraction were treated with red blood cell lysis buffer to remove red blood cells and with 0.25% trypsin-EDTA for 5 minutes at 37°C to yield a single cell suspension. Cells were maintained in DMEM containing 10% fetal bovine serum and 1% penicillin/streptomycin at 37°C with 5% CO_2.

RNA Sequencing

RNA sequencing data were obtained from Tao et al,[7] where 54 genes were identified to be differentially expressed between TAO and non-TAO OASCs. These genes were determined to be differentially expressed

Table 1. Clinical Summary

Diagnosis	Sex	Age	Thyroid Treatment	Smoking	Steroids	CON	CAS
TAO	Female	55	RAI, thyroidectomy	No	Oral	Y	4/7
TAO	Female	55	RAI, thyroidectomy	Previous	IV	N	[a]
TAO	Female	58	Thyroidectomy	No	IV	Y	4/7
Control	Female	77	N/A	No	N/A	N/A	N/A
Control	Male	82	N/A	Previous	N/A	N/A	N/A
Control	Female	54	N/A	No	N/A	N/A	N/A

CON, compressive optic neuropathy; IV, intravenous; N/A, not applicable; RAI, radioactive iodine.
[a]The CAS was not officially recorded; the patient had chemosis, injection, eyelid edema, and diplopia.

Table 2. Key DEGs

Gene Symbol	Gene Description	Log2 Fold Change	*P*-Value
IRX1	Iroquois homeobox protein 1	+4.24	1.97^{-13}
HOXB2	Homeobox B2	+3.32	1.19^{-5}
S100B	S100 Ca-binding protein B	+2.80	7.98^{-9}
KCNA4	Potassium voltage-gated channel A member 4	+2.57	3.50^{-7}

based on both EdgeR and DESeq2 software and demonstrated a *P* value of less than 0.005 and a fold change of greater than 1.5. Of these genes, IRX1, HOXB2, S100B, and KCNA4 were determined to be the most differentially expressed and thus were selected to be examined further in our study (Table 2).

LINCS L1000

The L1000 Characteristic Direction Signature Search Engine (L1000CDS^2) (http://amp.pharm.mssm.edu/L1000CDS2) was used to search for perturbagens that reverse the inputted OASC TAO gene expression signature.

Cell Viability Assay

OASCs from controls were seeded at a density of 5×10^3 cells/well in 96-well plates in 100 µL media. After 24 hours, OASCs were treated with Torin 2 (0.01–5.00 µM) (Selleckchem Catalog No. S2817; Selleckchem, Houston, TX), PX12 (0.5–40.0 µM) (Selleckchem Catalog No. S7947), withaferin A (0.05–10.00 µM) (Abcam CAS number 5119-48-2; Abcam, Cambridge, MA), isoliquiritigenin (0.5–50.0 µM) (Selleckchem Catalog No. S2404), mitoxantrone (0.01–5.00 µM) (Selleckchem Catalog No. S2485), and MLN8054 (0.5–50.0 µM) (Selleckchem Catalog No. S1100) for 72 hours. After treatment, 3-(4,5-dimethylthiazol-2-yl)-2, 5-diphenyltetrazolium bromide (MTT) assay (Biotium, Fremont, CA) was performed according to the manufacturer's instructions to measure the mitochondrial metabolism rate as an indicator for proliferation and viability. MTT (5 mg/mL) was added and plates were incubated at 37°C for 4 hours before dimethyl sulfoxide (100 µL) was added to each well. Upon verifying dissolution of the formazan salt, the absorbance of each well was read at a wavelength of 570 nm using a scanning multiwell spectrophotometer. The results of three identically treated, independent wells were averaged to yield corresponding cell viability measurements.

Adipogenesis Assay

OASCs during passages three to five were seeded at a density of 2.5×10^4 cells per cm^2 in 24-well PL plates in DMEM with 10% fetal bovine serum. At 90% confluence on day 3, the medium was switched to the Adipogenesis Differentiation Medium (Invitrogen, Carlsbad, CA). Torin 2 (0.02 µM), PX12 (10 µM), withaferin A (0.5 µM), isoliquiritigenin (25 µM), mitoxantrone (0.025 µM), and MLN 8054 (5 µM) were added 3 days after differentiation induction of OASC into mature adipocytes. After 21 days of culturing, the cells were fixed with 4% paraformaldehyde and stained with Oil Red O for adipocytes from the Adipogenesis Assay Kit (Cayman Chemical Company, Ann Arbor, MI) according to the manufacturer's protocol. Cells with oil droplets stained by Oil Red O were quantified via spectrophotometry at an absorbance of OD 490 nm in triplicate cultures (Fig. 1).

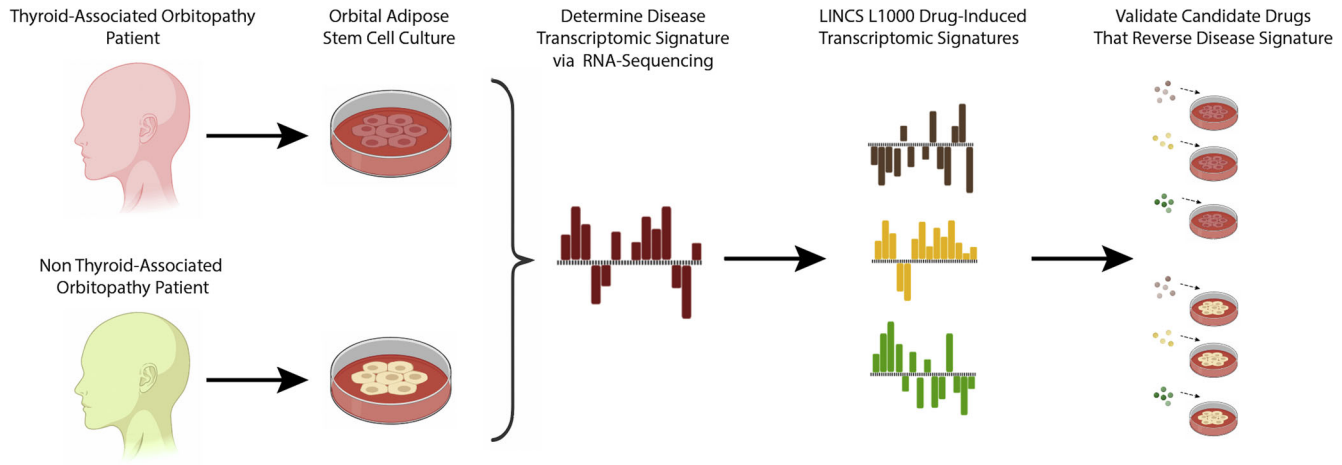

Figure 1. Study schematic diagram. OASC samples are isolated from patients with and without TAO. DEG is obtained by comparing transcriptomic signatures for TAO and non-TAO samples. LINCS L1000 outputs candidate drugs to reverse pathologic signature and are tested in vitro to determine drug efficacy.

Quantitative Real-Time Polymerase Chain Reaction

Quantitative real-time polymerase chain reaction analysis was performed using gene-specific primers: IRX1 (5′ GGGGCACTCAATGGAGACAA 3′ CCAGAGAGTTGTCGCGTACC), HOXB2 (5′ CTCCCCCTCCCAAAATCGC 3′ GGGAAGGTTTGCTCGAAAGG), S100B (5′ TGTAGACCCTAACCCGGAGG 3′ TGCATGGATGAGGAACGCAT), KCNA4 (5′ CGA CAGGGATCTCGTCATGG 3′ GTCAGTGCCCAGTGTGATGA), peroxisome proliferator activated receptor-γ (5′ GATACACTGTCTGCAAACATATCACAA 3′ CCACGGAGCTGATCCCAA), FABP4 (5′ TGGGCCAGGAATTTGACGAA 3′ CACATGTACCAGGACACCCC) and human β-actin (5′ CACCAACTGGGACGACAT 3′ ACAGCCTGGATAGCAACG). Relative expression was calculated using the standard curve method and normalized to housekeeping gene β-actin. Before quantitative polymerase chain reaction analysis, OASCs in the treatment group were cultured with respective drug concentrations for 7 days with drug and media change every 48 hours.

Statistical Analysis

Statistical analyses were performed with a one-tailed Student t-test with a confidence level of greater than 95%. A P value of less than .05 was deemed statistically significant. Graphic data are presented as mean ± standard deviation.

Results

Selecting Ideal Small Molecule Candidates from LINCS L1000 Output

Figure 2 displays a clustergram of the top small molecule candidates projected to best revert the 54 DEGs of TAO OASCs according to LINCS L1000CDS^2 output and delineates the predicted upregulation or downregulation of each drug with respect to each DEG. The complete list contains 50 individual small molecules (Supplementary Table S1).

Torin-2 (a mammalian target of rapamycin inhibitor), PX12 (a thioredoxin-1 inhibitor), withaferin A (a steroidal lactone), isoliquiritigenin (a flavonoid), mitoxantrone (a type II topisomerase inhibitor), and MLN-8054 (an aurora kinase inhibitor) were selected for testing based on (1) LINCS L1000CDS^2 rank, (2) potential synergistic mechanistic benefit with respect to TAO pathology, and (3) a specific gene target (Table 3).

LINCS-derived Molecules Reverse Key DEGs

Based on the results from Tao et al,[7] IRX1, HOXB2, S100B, and KCNA4 are a collection of the most differentially upregulated and potentially pathologically influential genes in TAO OASCs. The expression of these genes was significantly diminished following treatment of TAO OASCs ($n = 3$), with selected LINCS-derived small molecules (Fig. 3). The degree of differential gene expression is noted in Table 2. The expression levels of IRX1 (the most differentially upregulated gene), and KNCA4

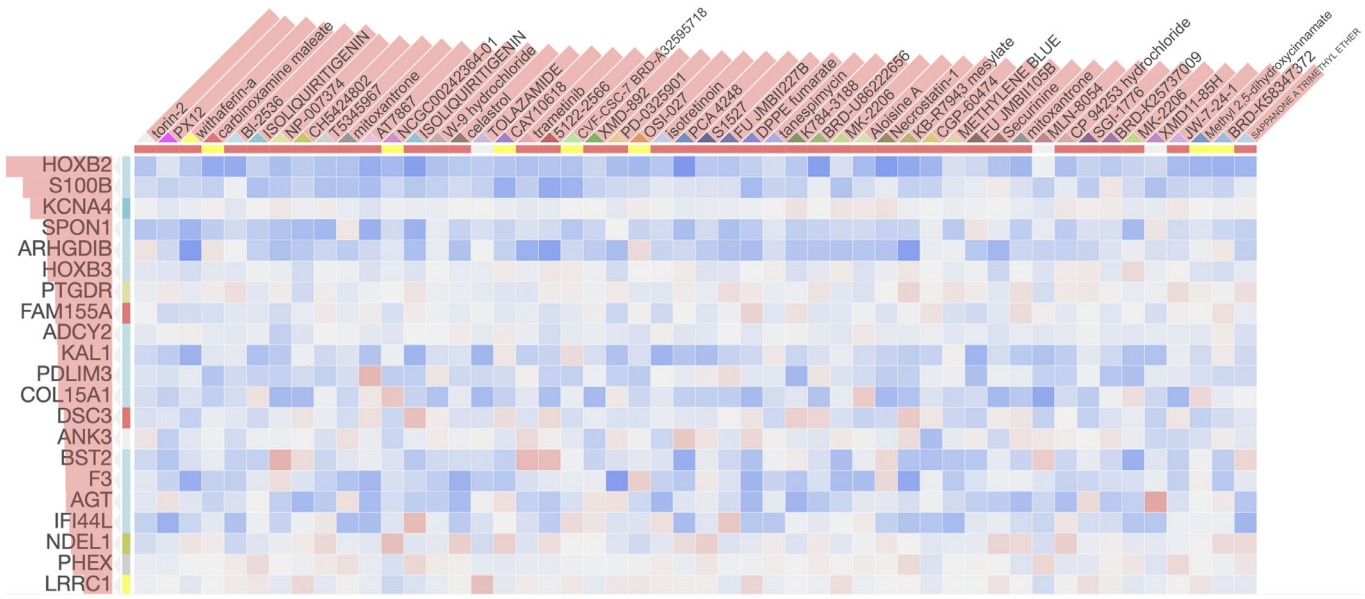

Figure 2. LINCS L1000CDS2 output. Clustergram of small molecules (*columns*) and DEGs (*rows*). *Blue colors* correspond with suppression of expression and *red colors* correspond with upregulation of expression.

Table 3. LINCS L1000CDS^2-Derived Drug Information

Rank	Drug Name	MOA	Notes
1	Torin-2	mTOR inhibitor	mTOR facilitates insulin-induced glucose uptake in adipocytes.
2	PX12	Trx-1 inhibitor	Trx-1 upregulates cell growth and inhibits apoptosis. PX12 is a strong HOXB2 modulator.
3	Withaferin A	Steroidal lactone (nuclear factor-κB inhibitor)	Inhibits adipogenesis, downregulates inflammation (TNF-α and IL-6).
6	Isoliquiritigenin	Flavanoid, inhibits aldose reductase	Suppresses adipose inflammation, suppresses saturated fatty acid synthesis.
10	Mitoxantrone	Type II Topoisomerase inhibitor	Antiproliferative effect in subconjunctival fibroblasts.
41	MLN-8054	Aurora kinase inhibitor	Strongest down-regulator of HOXB2.

MOA, mechanism of action; mTOR, mammalian target of rapamycin; TNF, tumor necrosis factor; Trx-1, thioredoxin-1.

were significantly decreased ($P < .05$) in three of the six small molecule treatment groups (isoliquiritigenin, mitoxantrone, and MLN-8054), although other groups demonstrated nonstatistically significant levels of reduction. Expression levels of HOXB2 was significantly reduced in five of six small molecule treatment groups (Torin 2, PX12, withaferin A, isoliquiritigenin, and MLN-8054). Likewise, expression levels of S100B was significantly reduced in five of the six small molecule treatment groups (Torin 2, PX12, isoliquiritigenin, mitoxantrone, and MLN-8054).

LINCS-derived Molecules Inhibit Adipogenic Capacity of OASCs

In the treated TAO OASC-derived adipocytes ($n = 3$), all six small molecules yielded a significant decrease ($P < .05$) in Oil Red O staining, signifying a decrease in lipid content. Figure 4B and C represent these relative absorbance levels after treatment (normalized to each biological sample's respective untreated group). Withaferin A, among all biological groups, demonstrated the most dramatic relative reduction in lipid content with a more

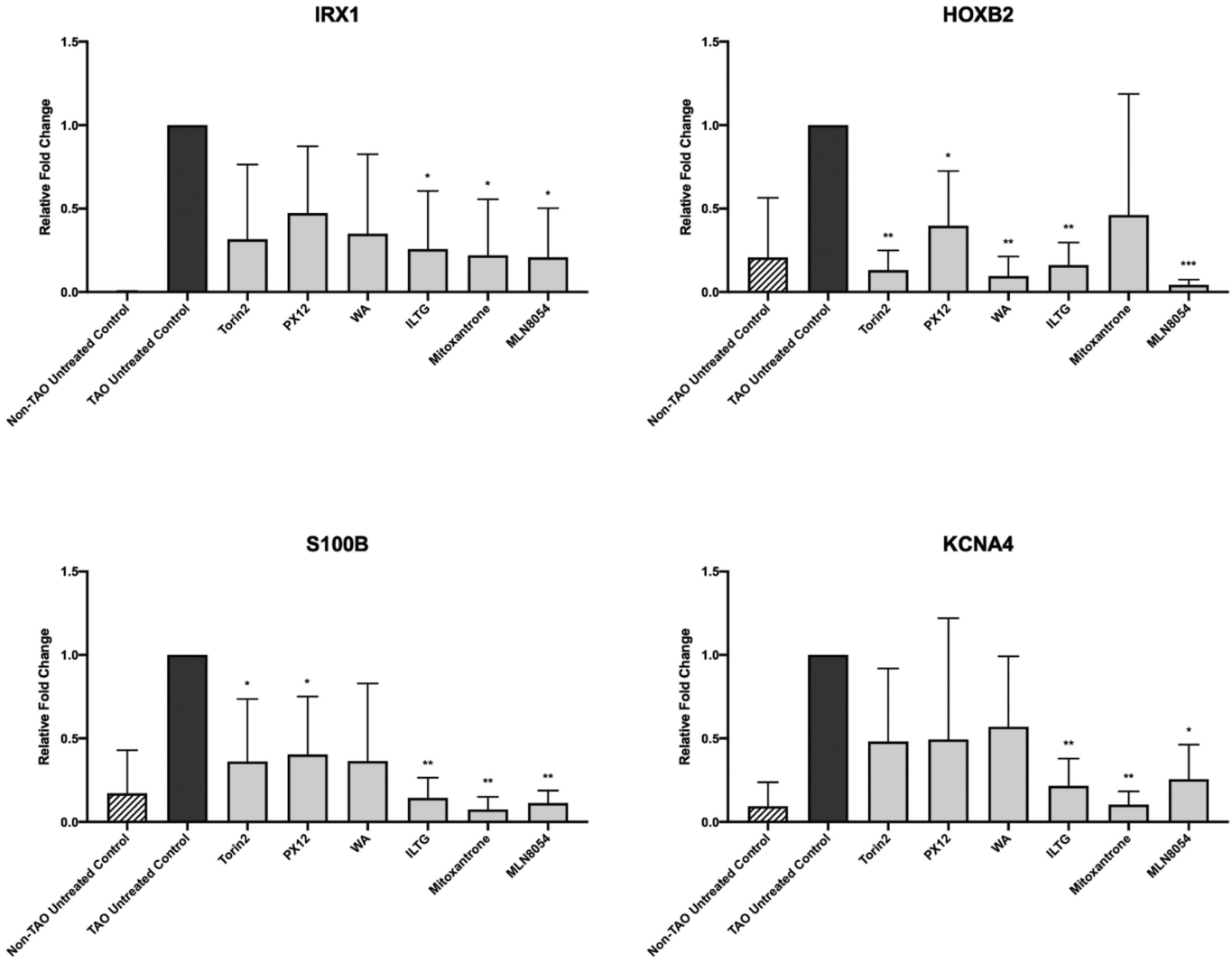

Figure 3. LINCS-derived small molecules reverse key DEGs. Real-time Polymerase Chain Reaction results demonstrating decreased expression of IRX1, HOXB2, S100B, and KCNA4 after treatment with small molecules. WA, withaferin A. Standard deviations are noted by error bars. *$P < 0.05$, **$P < 0.01$, ***$P < 0.001$.

than two-fold decrease. The MLN8054-treated groups demonstrated the smallest relative decrease in neutral lipid content (relative absorbance of 0.84; Fig. 4B).

In the treated non-TAO adipocytes ($n = 3$), three of six drugs (Torin 2, isoliquiritigenin, and mitoxantrone) yielded a significant reduction in Oil Red O staining ($P < .05$). In this group (treated non-TAO), withaferin A resulted in the most dramatic reduction in lipid content (relative absorbance of 0.66) but was not statistically significant owing to high variance. The MLN8054-treated groups yielded the smallest relative decrease in lipid content (relative absorbance of 0.91; Fig. 4C).

Between the treated TAO and treated non-TAO groups, the treated TAO groups resulted in a greater decrease in lipid content than in the treated non-TAO groups in all six drug treatment categories. Withaferin A treatment resulted in the greatest difference in relative lipid content between TAO and non-TAO treated cohorts, but was not statistically significant (difference = –0.23; Fig. 4). The mitoxantrone treatment group was the only group that reflected a statistically significant difference between treated TAO and treated non-TAO cohorts ($P < .05$; Fig. 4).

Expression levels of adipogenic genes were reduced in TAO OASCs after treatment (Fig. 4D). peroxisome proliferator activated receptor-γ expression was significantly decreased ($P < .05$) in TAO OASCs after treatment with torin-2 and mitoxantrone. FABP4 expression was significantly decreased in TAO OASCs after treatment with torin-2, PX12, and MLN8054.

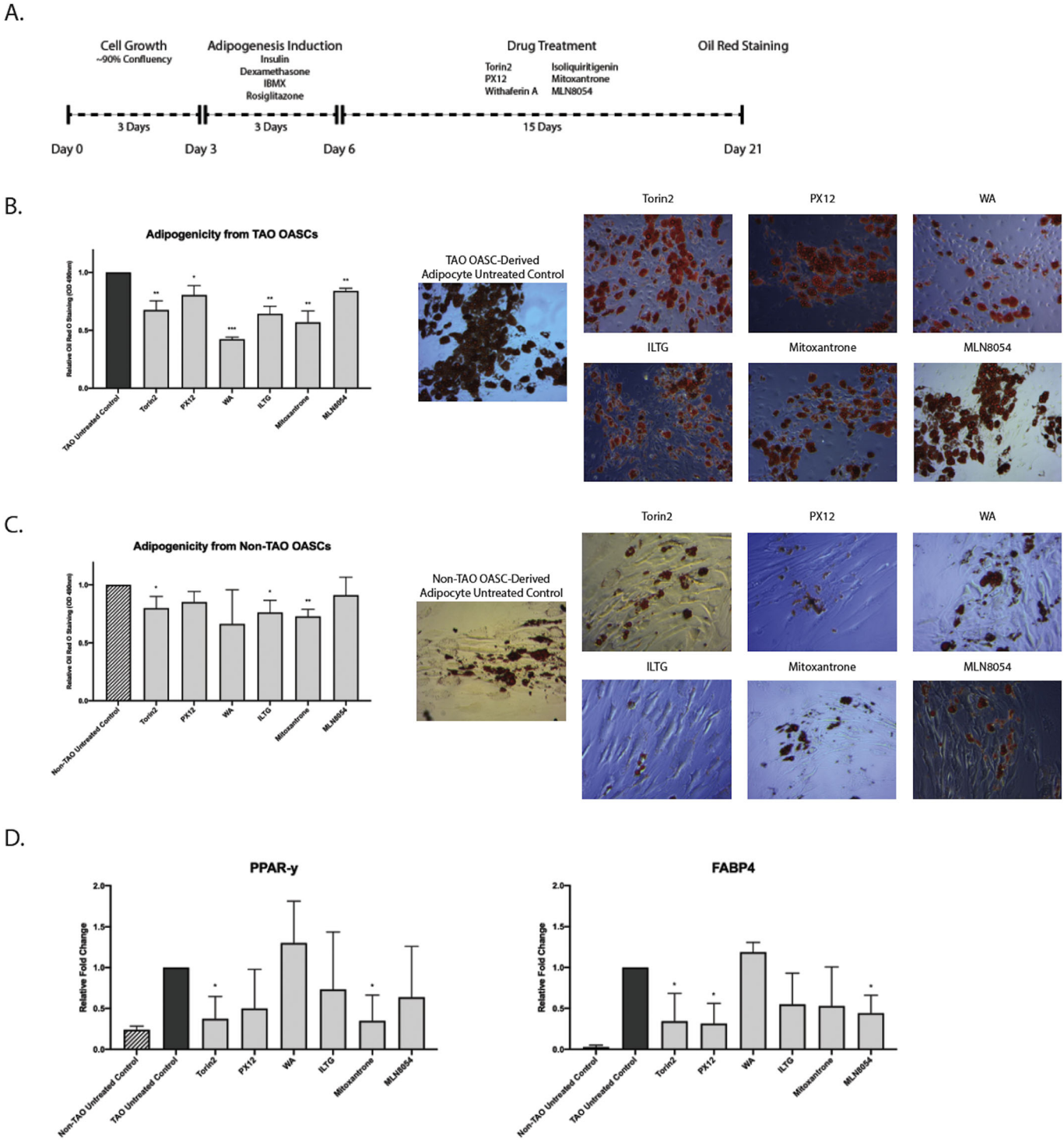

Figure 4. Treatment with LINCS-derived small molecules inhibits adipogenic capacity of TAO OASC-derived adipocytes. (A) Timeline of adipogenesis assay. (B) Quantification of Oil Red O assay and respective images showing inhibition of adipogenesis after treatment with LINCS-derived small molecules in TAO OASC-derived adipocytes. (C) Quantification of Oil Red O assay and respective images showing inhibition of adipogenesis after treatment with LINCS-derived small molecules in non-TAO OASC-derived adipocytes. (D) Real-time Polymerase Chain Reaction results demonstrating expression of adipogenic genes after treatment. $^{*}P < 0.05$, $^{**}P < 0.01$, $^{***}P < 0.001$.

After adipogenic induction, there were dramatic differences between untreated TAO and non-TAO controls, where images of untreated TAO adipocytes demonstrated larger, denser unilocular lipid droplets compared with the untreated non-TAO adipocytes. The OASC-derived adipocytes from TAO and non-TAO samples further demonstrated notable phenotypic changes after 15 days of treatment. After 15 days of small molecule treatment, TAO OASC-derived adipocytes demonstrated notably smaller, less dense, and multilocular lipid droplets compared with their corresponding untreated control TAO adipocytes (Fig. 4B). Likewise, the treated non-TAO OASC-derived adipocytes demonstrated less dense lipid aggregates but less pronounced differences in lipid size and locular structure since their respective untreated non-TAO control did not possess large, unilocular lipid structure to begin with (Fig. 4C).

Discussion

Justification for Selecting LINCS-derived Small Molecules

Aside from reverting expression of DEGs, our selected small molecules would ideally exhibit molecular activity that could synergistically target other pathologic mechanisms inherent to TAO. Inflammatory dysregulation, improper cellular proliferation and orbital adipogenesis, and tissue remodeling are fundamental pathologic processes that occur in patients with TAO. The orbital tissue activation and remodeling that occurs is attributed, in part, to proinflammatory cytokines, where cytokines such as TNF-α, IL-1β, interferon-γ, IL-4, IL-6, and IL-10 are found to be elevated in the orbital tissue and serum of patients with TAO.[15–18] These cytokines, along with thyroid-stimulating hormone receptor and insulin-like growth factor-1R stimulation, have critical roles in activating fibroblasts, stimulating B and T lymphocytes, and remodeling orbital tissue (adipocyte hyperplasia, extraocular muscle enlargement, and glycosaminoglycan overproduction). Thus, by carefully selecting small molecules that could dualistically target these various mechanisms while renormalizing DEGs, we would theoretically expect a greater chance of success if implemented in a clinical setting.

Torin-2, a mammalian target of rapamycin inhibitor, was the top ranked small molecule on our LINCS L1000CDS^2 drug list based on these selection criteria. In adipocytes, mammalian target of rapamycin activity has been linked to insulin-induced glucose uptake with inhibition of this process leading to adipocyte destruction.[19,20] PX12, a thioredoxin-1 inhibitor, was the second highest ranked small molecule. Thioredoxin-1 has been implicated in dysregulated cell growth and inhibition of apoptosis.[21] The role of this mechanism has not been studied in adipocytes or fibroblast cell types specifically, but a similar mechanistic process could play a role in the dysregulated adipocyte proliferation seen in thyroid eye disease. PX12 is also a strong downregulator of HOXB2, one of the most DEGs and suspected key genes in TAO pathogenicity, based on LINCS L1000CDS^2 cluster gram (Fig. 2). MLN-8054, an aurora kinase inhibitor, was selected as a drug candidate despite being ranked 41st on our L1000CDS^2 list, because it was predicted to have the strongest downregulatory effect on HOXB2.[22]

Withaferin A, a steroidal lactone, was our third ranked drug and an attractive candidate to study because of its synergistic mechanisms of inhibiting adipogenesis, downregulating inflammation (tumor necrosis factor-α and IL-6), and upregulating fat metabolism.[23] Inhibition of nuclear factor-κB by steroidal lactones is accredited for the anti-adipogenic properties of this drug. Similarly, isoliquiritegenin, a flavonoid and sixth ranked drug, has shown the ability to both suppress adipose tissue inflammation (tumor necrosis factor-α) and inhibit fatty acid synthesis.[24] Mitoxantrone, a type II topoisomerase inhibitor and the 10th ranked drug, was selected because of its antiproliferative effects in subconjunctival fibroblasts.[25]

Understanding the Relationship between Differential Gene Reversion and Inhibition of Adipogenicity

Although our data as a whole seemingly reflect a corresponding association with reversal of DEGs and suppression of adipogenicity, this phenomenon cannot be attributed to the effect of DEG reversion alone. As highlighted previously, we selected small molecules with mechanistic actions that could synergistically target other pathologic processes in TAO. For example, withaferin A was selected in our study because of its reported antiadipogenic and anti-inflammatory properties. Based on our gene reversion analysis, withaferin A exhibited dramatic effects on HOXB2 expression to near nonpathologic baseline levels, but failed to demonstrate a significant effect on IRX1, KCNA4, and S100B (Fig. 3). Furthermore, there was no decrease in the expression of adipogenic genes (Fig. 4D). Yet, in terms of its effects on adipocytes, it exhibited the most dramatic

reduction in neutral lipids (Fig. 4B). This phenomenon is likely not due to DEG renormalization, but to the inherent adipocyte toxicity of withaferin A. Withaferin A was the only small molecule in our study that demonstrated adipocyte toxicity at equivalent concentrations in certain biologic sample groups, contributing to a perceived greater effect on adipogenesis attenuation.

Likewise, MLN-8054 demonstrated significant alterations in all four DEGs with treatment, but yielded the least dramatic, albeit still significant, decrease in adipocyte lipid content. Thus, the overlapping role of our tested small molecules in both reversion of DEGs and effect on TAO pathologic mechanisms make it difficult to draw a clear correlation between the magnitude of DEG reversion and inhibition of adipogenicity. Although there may, in fact, be a causal relationship between DEG renormalization and attenuation of adipogenicity (or other TAO pathologic processes), one cannot draw a clear correlation between these factors without a better understanding of the specific role of each DEG in TAO pathophysiology and other non-DEG targets of our studied small molecules. Ongoing studies are needed to further clarify these factors.

Selectivity of LINCS-derived Small Molecules

Therapies that can selectively target pathologic cells while avoiding healthy cells are an ideal option to avoid the side effects and additional risks of treatment. Theoretically, LINCS-derived small molecules should exhibit some degree of selectivity to pathologic cell targets, because they are selected based on differential gene expression. Our adipogenicity data suggest that these drugs may, in fact, exhibit a degree of selectivity. In the pathologic TAO adipocyte group, there was a statistically significant reduction in adipogenicity with all 6 drug treatments, whereas the healthy non-TAO adipocyte group exhibited a significant decrease in only three of the six drug treatments alone (Fig. 4). At the same time, the relative decrease in adipogenicity that occurred in TAO adipocytes was consistently greater than in the non-TAO adipocytes, even though mitoxantrone alone exhibited a statistically significant difference in the magnitude of adipogenesis suppression between TAO and non-TAO treatment groups ($P < .05$). Although additional cell lines would provide better clarity to this phenomenon ($n = 3$ in each group in our study), the results of our study suggests that our selected small molecules may possess preferential efficacy in pathologic cells.

Implications and Limitations of Multigene Reversion

Our study was able to demonstrate reversal of multiple DEGs in treated TAO OASCs. The 4 DEGs measured in this study—IRX1, HOXB2, S100B, and KCNA4—were previously reported to be the most differentially upregulated genes in TAO OASCs based on RNA sequencing data.[7] However, our current study does not comprehensively examine the alteration in expression of all 54 DEGs noted in the aforementioned study. A comprehensive assessment of OASC gene expression alteration after treatment would provide additional information after this pilot study to evaluate alterations in DEGs after treatment.

In addition, LINCS-derived drugs are unable to affect all DEGs comprehensively. In fact, the expression of certain DEGs could possibly be altered to deviate even further from their nonpathologic baseline (Fig. 2). Each small molecule (columns) is predicted to either downregulate (blue) or upregulate (red) a DEG (rows). As apparent in the Figure 2 clustergram, it is difficult to identify a small molecule that can comprehensively renormalize each of the 54 DEGs appropriately (all 54 not shown). Although the expression of a DEG gene may be downregulated toward nonpathologic levels, the expression of another DEG may be upregulated to deviate even further from their nonpathologic baseline. The implications of this finding are that several nontarget genes may be activated or suppressed that may counteract the benefit that a drug may have on reversing pathologic TAO expression. Moreover, the clinical significance of each DEG is not yet well-characterized for TAO, and the differential expression of a gene does not necessarily correlate with greater clinical significance in terms of disease state. Likewise, a smaller alteration in the expression of one gene could have a greater impact than a larger alteration in another. Further studies that can help to elucidate the importance and role of each DEG in TAO pathogenesis would help to prioritize certain genes and filter a LINCS L1000CDS^2 output more specific to targeting these critical disease-altering genes.

Heterogeneity of TAO and Future Implications in Precision Medicine

Like many other diseases, TAO is a very heterogeneous disease with several classifications and categorizations. One way that TAO is categorized is based on disease severity, of which the European Group on Graves' orbitopathy CAS is most popularly used.[26] For an initial CAS, patients are given 1 point (out of

7) for each of the following parameters: spontaneous orbital pain, gaze evoked orbital pain, eyelid swelling considered to be due to active TAO, eyelid erythema, conjunctival redness considered to be due to active TAO, chemosis, and inflammation of caruncle or plica. Patients with a score of 4 of 7 or greater are considered to have active disease.

Another way that TAO is classified is by the primary tissue type responsible for orbital tissue expansion, where type I disease is characterized by adipose tissue enlargement and type II disease is characterized by extraocular muscle enlargement.[27] The clinical designation of this classification has shown to correlate cellularly, as type 1 orbital fibroblasts lead to a greater magnitude of adipocyte hyperplasia, and type II orbital fibroblasts typically demonstrate a greater proliferative response to inflammatory mediators.[28] Furthermore, these differences correlate with response to treatment, because only type II orbital fibroblasts were shown to respond to cyclooxygenase inhibition compared with type I counterparts.[28] Continuing studies that help further categorize TAO and understand the treatment implications based on these subcategories can help to provide more specialized treatment options for patients with TAO.

In the future, treatment options for TAO could potentially be even more precise. Certain samples respond better to certain drugs than others, because certain patients may respond better to certain drugs than others. Even in our study, the degree of DEG renormalization for each drug varied considerably for each biological sample (high standard deviation (SD); Fig. 3). The positive effects of drug treatment may still be exhibited in each sample, but could potentially be more efficacious if differential gene expression was measured for each sample/patient and compared independently with a universal healthy cell control (ideally averaging thousands of different non-TAO samples). Each sample/patient could have their own unique DEG profile inputted into LINCS L1000CDS^2 (or a similar perturbagen response prediction software) to reveal a personalized treatment regimen based on one's own unique gene expression signature.

Currently, this level of precision therapy is behind, because barriers in data, technology, and cost prevent the implementation of these methods. However, recent advancements have made this level of personalized medicine an ever more imminent reality. Rapid whole genome sequencing has dramatically improved in terms of cost, speed, and accuracy and is at the cusp of becoming a feasible routine medical test.[29,30] Particularly in the oncology arena, this precision-based approach is being studied extensively, where LINCS has been used to develop personalized treatment combinations and response profiles for individual tumors.[10] LINCS has already been used to identify preclinical drug candidates for colorectal cancer, prostate cancer, renal cell carcinoma, glioblastomas, and meningiomas, although several of these studies lack supporting evidence of drug efficacy, such as gene reversion data or pathologic phenotype changes.[10–12,31,32] To the authors' knowledge, our study is the first to use the LINCS perturbagen prediction software to identify preclinical drug candidates with proof of in vitro drug efficacy in a noncancer disease. Furthermore, our study is one of few to actually provide evidence of treatment-associated differential gene reversion and pathologic cell phenotype improvement (attenuation of adipogenesis). Incorporating these advancements in drug identification with modern genetic technology could revolutionize the way we treat TAO and other diseases in the future.

Future Directions

A better understanding of key DEGs in TAO, the role DEG expression and disease severity/subtype, and the optimal treatment options for these respective subtypes could lead to a more precise and efficacious strategy toward treating patients with TAO. One of the primary limitations of our study is small study size and evaluation of only patients with active disease. Although two out of three patients had CAS scores of 4 out of 7, one patient did not have an official CAS score recorded but did have chemosis, injection, eyelid edema, and diplopia suggestive of type II active disease. By sequencing more samples of TAO OACSs organized by CAS and type I/II classification, we may be able to identify key DEGs that are responsible for disease severity and cellular phenotype. Rerunning the LINCS L1000CDS^2 software after stratification of these parameters with larger patient numbers may help to identify small molecules that are more ideal preclinical treatment options for a respective TAO subtype.

Furthermore, our in vitro study model is limited because of its inability to grasp the full extent of TAO pathogenicity and heterogeneity. Upregulated adipogenicity is only one manifesting component of TAO. In addition to being immune isolated and cellularly homogenous, our model fails to capture the full effect of our tested LINCS-derived small molecules, which would require an in vivo assessment. Immunologic, intercellular, and external factors may also be affected by these small molecules but cannot be assessed by our in vitro model alone. A study that can implement these drugs in an in vivo TAO animal model would help to better characterize and validate their efficacy.

Conclusions

Our study demonstrates that combining disease-specific gene expression signatures with LINCS small molecule perturbagen-response profiles can identify promising preclinical drug candidates for TAO. Our LINCS-predicted drugs were able to re-normalize the expression of DEGs in TAO OASCs, exhibit correlating morphologic and adipogenic changes, and demonstrate preferential effect in diseased cells. These findings not only offer insight into future potential therapeutic options for TAO, but also highlight the potential of LINCs to elicit promising preclinical therapies in other diseases.

Acknowledgments

The Bascom Palmer Eye Institute is supported by NIH Center Core Grant P30EY014801, Research to Prevent Blindness Unrestricted Grant (New York, NY). This research was support by the above grant, private donor funding, the Nasser Ibrahim Al-Rashid Orbital Vision Research Fund, and Research to Prevent Blindness Medical Student Fellowship.

Disclosure: **J.Y. Lee,** None; **R.A. Gallo,** None; **P.J. Ledon,** None; **W. Tao,** None; **D.T. Tse,** None; **D. Pelaez,** None; **S.T. Wester,** Horizon Therapeutics (C)

References

1. Weetman AP. Graves' disease. *N Engl J Med*. 2000;343:1236–1248.
2. Bahn RS. Graves' ophthalmopathy. *N Engl J Med*. 2010;362:726–738.
3. Garrity JA, Bahn RS. Pathogenesis of graves ophthalmopathy: implications for prediction, prevention, and treatment. *Am J Ophthalmol*. 2006;142:147–153.
4. Smith TJ, Kahaly GJ, Ezra DG, et al. Teprotumumab for thyroid-associated ophthalmopathy. *N Engl J Med*. 2017;376:1748–1761.
5. Douglas RS, Kahaly GJ, Patel A, et al. Teprotumumab for the treatment of active thyroid eye disease. *N Engl J Med*. 2020;382:341–352.
6. The US Food and Drug Administration. FDA approves first treatment for thyroid eye disease. 2020. Available at: https://www.fda.gov/news-events/press-announcements/fda-approves-first-treatment-thyroid-eye-disease. Accessed February 1, 2020.
7. Tao W, Ayala-Haedo JA, Field MG, Pelaez D, Wester ST. RNA-sequencing gene expression profiling of orbital adipose-derived stem cell population implicate HOX genes and WNT signaling dysregulation in the pathogenesis of thyroid-associated orbitopathy. *Invest Ophthalmol Vis Sci*. 2017;58:6146–6158.
8. Koleti A, Terryn R, Stathias V, et al. Data portal for the library of integrated network-based cellular signatures (LINCS) program: integrated access to diverse large-scale cellular perturbation response data. *Nucleic Acids Res*. 2018;46:D558–D566.
9. Subramanian A, Narayan R, Corsello SM, et al. A next generation connectivity map: L1000 platform and the first 1,000,000 profiles. *Cell*. 2017;171:1437–1452.e1417.
10. Stathias V, Jermakowicz AM, Maloof ME, et al. Drug and disease signature integration identifies synergistic combinations in glioblastoma. *Nat Commun*. 2018;9:5315.
11. Huang YM, Cheng CH, Pan SL, Yang PM, Lin DY, Lee KH. Gene expression signature-based approach identifies antifungal drug ciclopirox as a novel inhibitor of HMGA2 in colorectal cancer. *Biomolecules*. 2019;9.
12. Zador Z, King AT, Geifman N. New drug candidates for treatment of atypical meningiomas: an integrated approach using gene expression signatures for drug repurposing. *PLoS One*. 2018;13:e0194701.
13. Korn BS, Kikkawa DO, Hicok KC. Identification and characterization of adult stem cells from human orbital adipose tissue. *Ophthalmic Plast Reconstr Surg*. 2009;25:27–32.
14. Chen SY, Mahabole M, Horesh E, Wester S, Goldberg JL, Tseng SC. Isolation and characterization of mesenchymal progenitor cells from human orbital adipose tissue. *Invest Ophthalmol Vis Sci*. 2014;55:4842–4852.
15. Smith TJ. Insights into the role of fibroblasts in human autoimmune diseases. *Clin Exp Immunol*. 2005;141:388–397.
16. Hiromatsu Y, Yang D, Bednarczuk T, Miyake I, Nonaka K, Inoue Y. Cytokine profiles in eye muscle tissue and orbital fat tissue from patients with thyroid-associated ophthalmopathy. *J Clin Endocrinol Metab*. 2000;85:1194–1199.
17. Molnar I, Balazs C. High circulating IL-6 level in Graves' ophthalmopathy. *Autoimmunity*. 1997;25:91–96.
18. Wakelkamp IM, Gerding MN, Van Der Meer JW, Prummel MF, Wiersinga WM. Both Th1- and Th2-derived cytokines in serum are elevated

in Graves' ophthalmopathy. *Clin Exp Immunol*. 2000;121:453–457.
19. Mullins GR, Wang L, Raje V, et al. Catecholamine-induced lipolysis causes mTOR complex dissociation and inhibits glucose uptake in adipocytes. *Proc Natl Acad Sci USA*. 2014;111:17450–17455.
20. Li H, Yuan Y, Zhang Y, Zhang X, Gao L, Xu R. Icariin inhibits AMPK-dependent autophagy and adipogenesis in adipocytes in vitro and in a model of graves' orbitopathy in vivo. *Front Physiol*. 2017;8:45.
21. Baker AF, Dragovich T, Tate WR, et al. The antitumor thioredoxin-1 inhibitor PX-12 (1-methylpropyl 2-imidazolyl disulfide) decreases thioredoxin-1 and VEGF levels in cancer patient plasma. *J Lab Clin Med*. 2006;147:83–90.
22. Sells TB, Chau R, Ecsedy JA, et al. MLN8054 and alisertib (MLN8237): discovery of selective oral aurora A inhibitors. *ACS Med Chem Lett*. 2015;6:630–634.
23. Khalilpourfarshbafi M, Devi Murugan D, Abdul Sattar MZ, Sucedaram Y, Abdullah NA. Withaferin A inhibits adipogenesis in 3T3-F442A cell line, improves insulin sensitivity and promotes weight loss in high fat diet-induced obese mice. *PLoS One*. 2019;14:e0218792.
24. Watanabe Y, Nagai Y, Honda H, et al. Isoliquiritigenin attenuates adipose tissue inflammation in vitro and adipose tissue fibrosis through inhibition of innate immune responses in Mice. *Sci Rep*. 2016;6:23097.
25. Maignen F, Tilleul P, Billardon C, et al. Antiproliferative activity of a liposomal delivery system of mitoxantrone on rabbit subconjunctival fibroblasts in an ex-vivo model. *J Ocul Pharmacol Ther*. 1996;12:289–298.
26. Bartalena L, Baldeschi L, Dickinson A, et al. Consensus statement of the European Group on Graves' orbitopathy (EUGOGO) on management of GO. *Eur J Endocrinol*. 2008;158:273–285.
27. Wang Y, Smith TJ. Current concepts in the molecular pathogenesis of thyroid-associated ophthalmopathy. *Invest Ophthalmol Vis Sci*. 2014;55:1735–1748.
28. Kuriyan AE, Woeller CF, O'Loughlin CW, Phipps RP, Feldon SE. Orbital fibroblasts from thyroid eye disease patients differ in proliferative and adipogenic responses depending on disease subtype. *Invest Ophthalmol Vis Sci*. 2013;54:7370–7377.
29. Miller NA, Farrow EG, Gibson M, et al. A 26-hour system of highly sensitive whole genome sequencing for emergency management of genetic diseases. *Genome Med*. 2015;7:100.
30. Farnaes L, Hildreth A, Sweeney NM, et al. Rapid whole-genome sequencing decreases infant morbidity and cost of hospitalization. *NPJ Genom Med*. 2018;3:10.
31. Kim IW, Kim JH, Oh JM. Screening of drug repositioning candidates for castration resistant prostate cancer. *Front Oncol*. 2019;9:661.
32. Koudijs KKM, Terwisscha van Scheltinga AGT, Bohringer S, Schimmel KJM, Guchelaar HJ. Personalised drug repositioning for clear cell renal cell carcinoma using gene expression. *Sci Rep*. 2018;8:5250.